Nonfouling, Encoded Hydrogel Microparticles for Multiplex MicroRNA Profiling Directly from Formalin-Fixed, Paraffin-Embedded Tissue

Citation: Nagarajan, Maxwell Benjamin et al. "Nonfouling, Encoded Hydrogel Microparticles for Multiplex MicroRNA Profiling Directly from Formalin-Fixed, Paraffin-Embedded Tissue." Analytical Chemistry 90, 17 (August 2018): 10279-10285 © 2018 American Chemical Society

As Published: http://dx.doi.org/10.1021/acs.analchem.8b02010

Publisher: American Chemical Society (ACS)

Persistent URL: https://hdl.handle.net/1721.1/125269

Version: Author's final manuscript: final author's manuscript post peer review, without publisher's formatting or copy editing

HHS Public Access

Author manuscript

Anal Chem. Author manuscript; available in PMC 2019 September 04.

Published in final edited form as:

Anal Chem. 2018 September 04; 90(17): 10279–10285. doi:10.1021/acs.analchem.8b02010.

Non-fouling, encoded hydrogel microparticles for multiplex microRNA profiling directly from formalin-fixed, paraffin-embedded tissue

Maxwell B. Nagarajan[†], **Augusto M. Tentori**[†], **Wen Cai Zhang**[‡], **Frank J. Slack**[‡], and **Patrick S. Doyle**[*,†]

[†]Department of Chemical Engineering, Massachusetts Institute of Technology, Cambridge, Massachusetts, 02139, USA

[‡]HMS Initiative for RNA Medicine, Department of Pathology, Beth Israel Deaconess Medical Center, Harvard Medical School, 330 Brookline Avenue, Boston, Massachusetts, 02215, USA

Abstract

MicroRNAs (miRNA) are short, non-coding RNAs that have been implicated in many diseases, including cancers. Because miRNAs are dysregulated in disease, miRNAs show promise as highly stable biomarkers. Formalin-fixed, paraffin-embedded (FFPE) tissue is a valuable sample type to assay for biomolecules because it is a convenient storage method and is often used by pathologists for histological staining. However, extracting biomolecules from FFPE tissue is challenging because of the presence of cellular and extracellular proteins, formaldehyde crosslinks, and paraffin. Moreover, most protocols to measure miRNA in FFPE tissue are time-consuming and laborious. Here, we report a simple protocol to directly measure miRNA from formalin-fixed cells, FFPE tissue sections after paraffin is removed, and FFPE tissue sections using encoded hydrogel microparticles fabricated using stop flow lithography. Measurements by these particles show agreement between formalin-fixed cells and fresh cells, and measurement of FFPE tissue with paraffin is 10% less than FFPE tissue when paraffin is removed before the assay. When normal and tumor FFPE tissue are compared using this microparticle assay, we observe differential miRNA signal for oncogenic miRNAs and tumor suppressing miRNAs. This approach reduces assay times, reduces the use of hazardous chemicals to remove paraffin, and provides a sensitive, quantitative, and multiplexed measurement of miRNA in FFPE tissue.

MicroRNAs (miRNAs) are small, non-coding RNAs[1] that are emerging as promising biomarkers because they have been shown to be dysregulated in many diseases, including cancers, and have high stability compared to other biomolecules.[2–5] However, quantifying miRNAs is challenging because miRNAs represent a small fraction (0.01%) of total RNA

[*]**Corresponding Author** pdoyle@mit.edu (P.S.D.).

Supporting Information

The Supporting Information is available free of charge on the ACS Publications website.

A list of reagents, additional supporting tables and figures, and a description of statistical methods are available as noted in the text (PDF).

Notes

The authors declare no competing financial interest.

mass, their melting temperature varies with GC content, and different miRNAs can differ by single nucleotides.[6,7] Existing techniques, including quantitative reverse transcription polymerization chain reaction, DNA microarrays, and sequencing technologies, have high sensitivity, but they come up short in categories relevant to clinical diagnostic applications, such as multiplexing capacity, quantitation without sequence bias caused by target amplification, and/or assay duration.[6,8,9] Moreover, existing techniques often require the isolation of total RNA from a sample before measuring miRNA, involving time-consuming separation techniques.[6]

Formalin-fixed, paraffin-embedded (FFPE) tissue is a valuable sample type to assay for biomolecules because it is currently used by pathologists, it is a convenient storage method, it is possible to cut into thin sections, and there is the potential to assay samples from the same patient over time. Moreover, paraffin tissue blocks have been collected for more than a century and include many diseases.[10] However, it is difficult to extract mRNA from these specimens because formaldehyde crosslinks mRNA to other biomolecules, leading to transcript fragmentation during tissue decrosslinking.[10,11] MiRNA expression profiles from FFPE tissue closely correlate with matched frozen specimens, indicating that miRNA do not fragment during tissue decrosslinking,[12–15] which has spurred interest in studying miRNA in FFPE tissue samples.[16–19] Still, extracting miRNAs from FFPE tissue is challenging because of the presence of cellular and extracellular proteins, formaldehyde crosslinks, and paraffin, and most methods to detect miRNA in FFPE tissue involve a long workflow of first removing paraffin, second removing the formaldehyde crosslinks, third isolating total RNA, and finally measuring miRNA expression levels.[14]

Polyethylene glycol (PEG) hydrogel microparticles have been used to measure biomolecules from complex samples with minimal sample prep in previous work from total tumor RNA,[20] human serum,[21] and raw cell lysate.[22] PEG hydrogels also provide a non-fouling scaffold for solution-like binding kinetics between the probe and target biomolecules.[23] We used stop flow lithography (SFL)[24] to polymerize individual PEG microparticles with a probe region to quantify a specific miRNA, a code region to identify which miRNA the particle is detecting, and internal negative control regions.[20–22,25] This barcode design allows for more than 1,000 distinct codes, more than is needed for a particular diagnostic experiment. 12-plex assays have been demonstrated in previous work, with all twelve different particle types included in the same tube with the sample.[20] Diagnostic potential for certain diseases has been shown using miRNA library sizes of thirteen,[26] seven,[27,28] five,[29] and three.[30] Thus, this platform is well-equipped to handle a sufficient amount of multiplexing for diagnostic uses.

In this paper, we use encoded hydrogel microparticles to quantify miRNA directly from several formalin-fixed samples: formalin-fixed cells, FFPE tissue with paraffin removed, and FFPE tissue. We show agreement between frozen and fixed cells and we identify a 10% reduction in overall assay signal in FFPE tissue compared to the case when paraffin was removed before the assay. We also observe differential miRNA signal for oncogenic miRNAs and tumor suppressing miRNAs when comparing FFPE non-small cell lung cancer tissue and FFPE normal lung tissue. This approach fits into the pathologist's workflow

because the same starting material for typical pathological stains can be used for this assay with no additional sample preparation.

EXPERIMENTAL SECTION

Particle Synthesis.

Particles were synthesized using stop flow lithography, as previously described.[20,22,24,31] Four monomer streams were coflowed through a polydimethylsiloxane (PDMS) microchannel (height ~ 40 μm) to generate particles with four regions: (1) a barcode region that was copolymerized with rhodamine acrylate for visualization of the particle barcode, (2) an inert region that acted as an internal negative control, (3) a probe region which contained a DNA probe complementary to a miRNA of interest, and (4) a second inert region. The monomer solutions contained polyethylene glycol diacrylate (PEG-DA) MW 700 g/mol as monomer, polyethylene glycol (PEG) MW 200 g/mol as porogen, Darocur 1173 as UV-activated photo initiator, and 1xTris-EDTA (1xTE) buffer. We flowed the monomer solution through the channel using compressed air, stopped the flow, and transmitted ultraviolet light (Thorlabs, 365 nm LED, 720 mW/cm^2, 100 ms exposure time) through a mylar photomask (Fineline, designed in AUTOCAD) placed in the field stop of the microscope and through a 20x objective. Code and inert regions of the particles were composed of 35% PEG-DA diluted 9:1 with either rhodamine acrylate or color dye for stream visualization, and the probe region of the particles was composed of 20% PEG-DA diluted 9:1 with DNA probe solution. The full compositions of the four monomer streams are shown in Table S1. After particles were formed, they were removed from the channel and washed in 1xTET (1xTris-EDTA buffer with 0.05% Tween 20) three times. In each wash step, 500 μL of 1xTET is added, tubes are vortexed for five seconds, tubes are centrifuged for 20 seconds, and 500 μL of supernatant is removed.

$KMnO_4$ was added to 0.1 M Tris-HCl (pH 8.8) to make a 600 μM solution. Particles were oxidized by adding 1 mL of $KMnO_4$ solution to 100 μL of particles in 1xTET and vortexing for 2 minutes. Particles were then washed in 1xTET three times.

Cell Fixation.

Human lung cancer cell line Calu-6 was cultured in Dulbecco's modified eagle medium with 10% fetal bovine serum, 2 mM L-glutamine, and 1% penicillin-streptomycin. Single cells were frozen with dimethyl sulfoxide in complete culture medium. Cells were kept in liquid nitrogen for long-term storage and −80 °C freezer for short-term storage. Before use, cells were thawed in room temperature media. Cells were fixed in paraformaldehyde by suspending cells in 1 mL of 4% paraformaldehyde in 1xPBS for 20 minutes. Fixed cells were then washed in 1xPBS and stored at 4 °C.

Animal Studies.

All research involving animals complied with protocols approved by the Beth Israel Deaconess Medical Center Institutional Animal Care and Use Committee. 4–6 weeks old female NU/J (Nude) immunodeficient mice (Jackson Laboratory #002019) were used for subcutaneous injections. 100,000 A549 cells in serum-free medium and growth factor

reduced Matrigel (Corning #354230) (1:1) were inoculated into the flank of nude mice. The xenograft tumor formation was monitored by calipers twice a week. The recipient mice were monitored and euthanized when the tumors reached 1 cm in diameter. The tumor tissues from four transplanted mice were isolated and were processed for paraffin block preparation.

K-ras$^{LSL\text{-}G12D/+}$; *p53*$^{fl/fl}$ (KP) genetically engineered mouse model for non-small cell lung cancer was established at the Beth Israel Deaconess Medical Center as reported previously.[32] In the same mouse lung, the tumor nodules and the far normal lung tissues, which are 1 cm away from tumor margins, were isolated and were processed for paraffin block preparation.

FFPE Tissue Preparation and H&E Staining.

All the tissues at 5 mm x 5 mm (length x width) were fixed in 4% paraformaldehyde for 24–48 hours. After fixation, the tissues were dehydrated with ethanol and xylene. Then the tissues were embedded into paraffin blocks. 5 μm sections of paraffin-embedded tissue were cut and placed onto glass microscope slides (Gold Seal). For hematoxylin and eosin (H&E) staining, the sections were stained with Hematoxylin and Eosin Y (Vector), dehydrated and then covered with mounting medium (Vector). The images were taken under a microscope (Olympus).

Tissue Handling.

For some FFPE tissue experiments, paraffin was removed before the assay, similar to a commercial protocol.[33] Tissue sections were removed from a slide by scraping with a scalpel and placing in a tube with ethanol. A new scalpel edge was used for each tissue section. Tubes of ethanol and tissue were vortexed and centrifuged at 10.0 RCF (relative centrifugal force) for 2 minutes to prevent the tissue from sticking to the sides of the tube. Ethanol was removed from the tube and 1 mL xylene was added to each tube. Tubes were vortexed for 15 seconds, centrifuged for 2 minutes at 10.0 RCF, and then heated at 50 °C for 3 minutes to melt the paraffin. The tubes were then vortexed for 15 seconds and centrifuged for 2 minutes at 10.0 RCF. The xylene was then removed. The tubes were washed in ethanol twice by adding 1 mL of ethanol, vortexing for 15 seconds, and centrifuging for 2 minutes at 10.0 RCF. After removing supernatant ethanol, the tubes were left out in a fume hood to dry for one hour. In other tissue experiments, FFPE tissue was added directly to tubes without the need for ethanol or xylenes.

MiRNA Assay Protocol.

The assay for miRNA quantification from cell lysate, fixed cells, and FFPE tissue is split into four steps: 1) formalin crosslink degradation, 2) miRNA hybridization, 3) ligation, and 4) labeling (Figures 1A and 1B). 1) To remove the formalin crosslinks, cells or tissue in 33 μL of 1xTET buffer containing 2% SDS and 8–32 U/mL proteinase K were heated at 50 °C for 15 minutes and 80 °C for 15 minutes (similar to a commercial protocol[33]) in a thermoshaker (MultiTherm Shaker, Thomas Scientific) at 1500 RPM. 2) As described previously,[20,22] particles were added and the NaCl concentration was increased to 350 mM to promote DNA-miRNA hybridization in a volume of 50 μL. The samples were heated to 55 °C for 90 minutes at 1500 RPM. These salt and temperature conditions have been used

previously to quantify many miRNAs.[20–22,34–36] Approximately forty particles per miRNA target were added to each sample.

While a larger sensing area may lead to a lower signal,[36,37] there need to be enough particles to easily collect and analyze them at the end of the assay. Following this step, the particles were washed three times in wash buffer (50 mM NaCl in 1xTET) by adding 500 μL to 50 μL of solution, vortexing, centrifuging, and then removing 500 μL from the supernatant. These washing steps are done to dilute the hybridization solution contents by a factor of 1000. By doing so, we did not observe any proteinase K activity in remainder of the assay. 3) A ligation solution was prepared with 40 nM biotinylated linker sequence, 800 U/mL T4 DNA ligase, 250 μM ATP, 1xNEBuffer 2, and 1xTET. 235 μL of ligation solution was added to the 50 μL particle solution and mixed in a thermoshaker for 30 minutes at 21.5 °C. During this step, the linker sequence hybridizes to the probe sequences and is ligated to miRNA bound to probe. Excess linker sequence is washed away during three wash steps in wash buffer. 4) In the labeling step, particles were incubated with 1.8 μg/mL streptavidin R-phycoerythrin (SAPE) in 1xTET and 50 mM NaCl for 45 minutes at 21.5 °C. After a final three wash steps in wash buffer, particles were imaged through a filter cube (Omega Optical XF101–2) on a Zeiss Axio Observer A1 microscope with a 20X objective, an Andor Clara CCD camera and Andor SOLIS software. The standard deviation of an assay result was calculated using 4–8 particles.

Image Analysis.

Images were analyzed using ImageJ.[38] ImageJ was used to rotate particles and determine the average fluorescence intensity in the probe region of the particle. The net signal was calculated by subtracting the average fluorescence intensity in the probe region of a particle from the average fluorescence intensity in the probe region of negative control particles. As in prior work,[20,22] the limit of detection (LOD) was defined as the amount of miRNA required to generate a signal three times the standard deviation of the negative control, when the signal to noise ratio (SNR) equals three. This was determined by generating a linear regression equation for log scaled data and finding the point where the signal was three times the standard deviation of the negative control. Using this approach, a lower limit of detection can be calculated in terms of the amount of miRNA and the number of cells.

RESULTS AND DISCUSSION

Evaluating assay performance with synthetic miRNA.

Assay performance of the hydrogel microparticles was determined by adding different amounts of synthetic miRNA to tubes containing miRNA-detecting hydrogel microparticles. MiRNA binds to DNA probes copolymerized within the probe regions of the particles. Biotinylated linker and DNA ligase are added to attach a biotin to each location of miRNA binding. SAPE binds to the biotinylated linker and allows fluorescent quantification in the probe regions of the particles. These data were used to generate a calibration curve for miR-21, a highly expressed miRNA that has been linked to several cancers, including non-small cell lung cancer[39–41] (Figure 1C). The lower limit of detection (LLOD) was determined by locating where the signal to noise ratio (SNR) equals three, which in this case

is 2.0 amol. Example particles from the calibration curve assays are shown in Figure 1D. The limits of detection of other miRNAs used in this work are shown in Table S2.

Multiplexed miRNA quantification from frozen and fixed cells.

Different from previous work with these hydrogel microparticles,[20,22] here the particles are first oxidized using $KMnO_4$, which was shown to reduce nonspecific binding of proteins to the particles by oxidizing unpolymerized double bonds.[34] We have found that oxidizing with $KMnO_4$ both increases the total assay signal in a cell assay and reduces nonspecific binding of cellular proteins to the hydrogel (Figure S1).

Before our goal of using the hydrogel microparticles to quantify miRNA in FFPE non-small cell lung cancer tissue, we first used hydrogel microparticles to quantify miRNA in Calu-6 cells, a non-small cell lung cancer cell line. Frozen Calu-6 cells were added directly to a tube with microparticles and lysis buffer to quantify miR-21 (Figure 2A). SDS and proteinase K were included in the hybridization buffer when quantifying miRNA from frozen cells to lyse membranes and degrade proteins complexed with miRNA, as was done previously.[22] The limit of detection found here was approximately 700 cells, in close agreement with previous results of 850 NIH 3T3 cells measured in previous work.[22] We then fixed these cells in paraformaldehyde and stored them at 4 °C for up to 300 days. To quantify miRNA from formalin-fixed cells, SDS and proteinase K were added to the cells, and the mixture was heated to 50 °C for 15 minutes and 80 °C for 15 minutes to remove formaldehyde crosslinks. We then added hybridization buffer and particles for miRNA quantification (Figures 2A and 2B). There is not a statistically significant difference between the miRNA signal measured per cell in fixed and frozen cells ($P = .18$) (Figure 2A), and the signal measured from 10,000 cells 300 days after fixation is only 15% less than the initial measurement (Figure 2B). These results indicate that the miRNA were well preserved in the cells during the fixation step and well preserved over time. Other recent work also shows that miRNA are well-preserved in and efficiently extracted from formalin-fixed cells and tissue.[11–15]

The barcodes on the hydrogel particles enable multiplexing. Using particles targeting two oncogenic miRNAs (miR-21 and miR-155),[40,42] two tumor suppressing miRNAs (let-7a and miR-34a),[2,43] and one control miRNA from *C. elegans* that has been previously used as a control (*cel*-miR-54),[22] we obtained a multiplexed measurement from Calu-6 cells (Figure 2C). Representative particles are shown in Figure 2D. The code regions of the particles in Figure 2D have different signal intensities because different amounts of rhodamine acrylate were in the monomer solutions during fabrication. The signal for *cel*-miR-54 was below the LOD of the assay.

Multiplexed miRNA quantification from FFPE tissue.

After demonstrating miRNA quantification from fixed cells, we used the encoded hydrogel microparticles to detect miRNA from FFPE tissue. We scraped FFPE tissue sections (~5 μm thick) off slides and placed them in tubes. In one experiment, tissue was washed in xylene to remove paraffin, tissue was heated with proteinase K and SDS as done for formalin-fixed cells, and then particles were added to extract miRNA. In a second experiment, proteinase K

and SDS were added directly to the FFPE tissue for formaldehyde crosslink removal, and then particles were added to the sample containing paraffin (Figure 3). We found that the signal for miR-155 in these samples was below the limit of detection for the assay. We also added an additional target, miR-210, a marker for hypoxia in tissue.[44] The signal from the particles with paraffin is only about 10% less than the signal from particles when paraffin was removed first. Over several separate experiments, this approach shows no more than 12% difference between a measurement with paraffin removed and one with paraffin (Figure S2). Some differences between samples are expected given biological variations between different sections of tissue. This demonstrates the utility of these non-fouling hydrogels for miRNA detection in FFPE tissue. Assaying the FFPE tissue directly is a substantial improvement over other methods of measuring miRNA from FFPE tissue, which generally involve removing paraffin, degrading the formaldehyde crosslinks, separating nucleic acids, isolating total RNA, and finally measuring miRNA. Not only does this method save time and reduce the number of assay steps, this approach also removes the need for working with the hazardous chemical xylene to remove the paraffin.

Proteinase K was added to the hybridization step of the assay to degrade the formaldehyde crosslinks by breaking up proteins inside the FFPE tissue. To optimize the assay with respect to the concentration of proteinase K, different concentrations of proteinase K were added to different tubes containing tissue sections, and the miR-21 signal was measured after completion of the miRNA assay (Figure 4). Synthetic *cel*-miR-54 was added as a positive control to determine if the presence of proteinase K and FFPE tissue affected the overall assay performance, independent of miRNA extraction efficiency or amount of miRNA in a tissue section. The signal from *cel*-miR-54 is about 15% less in the presence of tissue and proteinase K, further demonstrating small losses in the presence of paraffin and formaldehyde-crosslinked biomolecules. The 16 U/mL group has statistically significantly greater miR-21 signal than the 8 U/mL and 32 U/mL groups ($P < .001$ from a one-way analysis of variance followed by a Tukey honest significant difference test), and this increase in miR-21 signal is greater than the measured biological variations from proximal tissue sections (Figure S2).

We compared paired lung tissue sections from the same mouse in *K-ras*; *p53*-driven genetically engineered mouse models of non-small cell lung cancer. The tumor tissues from the tumor nodules form an adenocarcinoma-like structure with a great degree of cellular pleomorphism and nuclear atypia, while the normal lung tissue, which is 1 cm away from the tumor margin, forms a normal alveoli structure with air sacs surrounded by alveolar epithelial cells (Figure 5A). To quantify miRNA from these samples, we placed five tissue sections of FFPE tumor tissue sections and twenty tissue sections of FFPE normal tissue sections into tubes to give roughly equal tissue volumes (the area of tissue on the normal tissue section was about 4 times smaller than the area of the tumor tissue section, see Figure S3). We normalized the assay results by tissue volume. We did not remove paraffin before the assay, noting that there is much more paraffin in these tubes than for the previous experiments which had one section per tube. In tumor tissue, we observe greater expression of miR-21 ($P < .001$), an oncogenic miRNA in non-small cell lung cancer,[40] while in normal tissue, we observe greater expression of let-7a and miR-34a ($P < .001$), tumor suppressing miRNAs in non-small cell lung cancer (Figure 5B and C).[2,43] We do not observe a statistical

difference between the two tissue types in terms of expression of miR-210, a marker for hypoxia.[44]

CONCLUSIONS

Here we present a method to quantify miRNA directly from FFPE tissue using encoded hydrogel microparticles. The non-fouling nature of the hydrogels enables a direct measurement without laborious sample prep required in other approaches. This approach also does not require the use of xylene, a hazardous chemical used to deparaffinize FFPE tissue. We envision this technology as an addition to the pathologist's toolbox, in that proximal tissue sections can be used for existing histological stains and quantitative miRNA assays.

Supplementary Material

Refer to Web version on PubMed Central for supplementary material.

ACKNOWLEDGMENTS

This work was supported by The Bridge Project, a partnership between the Koch Institute for Integrative Cancer Research at MIT and the Dana-Farber/Harvard Cancer Center, and partially by Cancer Center Support (core) Grant P30-CA14051 from the National Cancer Institute. The authors also gratefully acknowledge research funding support from an NIGMS/NIH Interdepartmental Biotechnology Training Program Fellowship (M.B.N.), a Ford Foundation Postdoctoral Fellowship (A.M.T.), a Ludwig Center Fund Postdoctoral Fellowship (A.M.T.), NIH-NRSA 5T32HL007893-20 (W.C.Z), the NIH-YALE SPORE in Lung Cancer P50CA196530-03S1 (FJS), and NIH-NIBIB Grant 5R21EB024101-02 (P.S.D).

REFERENCES

(1). Bartel DP MicroRNAs: Genomics, Biogenesis, Mechanism, and Function. Cell 2004, 116, 281–297. [PubMed: 14744438]

(2). Esquela-Kerscher A; Slack FJ Oncomirs - microRNAs with a Role in Cancer. Nat. Rev. Cancer 2006, 6 (4), 259–269. [PubMed: 16557279]

(3). Calin GA; Croce CM MicroRNA Signatures in Human Cancers. Nat. Rev. Cancer 2006, 6 (11), 857–866. [PubMed: 17060945]

(4). Melo SA; Esteller M Dysregulation of microRNAs in Cancer: Playing with Fire. FEBS Lett 2011, 585 (13), 2087–2099. [PubMed: 20708002]

(5). Chen P-S; Su J-L; Hung M-C Dysregulation of MicroRNAs in Cancer. J. Biomed. Sci 2012, 19 (1), 90. [PubMed: 23075324]

(6). Pritchard CC; Cheng HH; Tewari M MicroRNA Profiling: Approaches and Considertions. Nat. Rev. Genet 2012, 13 (5), 358–369. [PubMed: 22510765]

(7). Baker M MicroRNA Profiling: Separating Signal from Noise. Nat. Methods 2010, 7 (9), 687–692. [PubMed: 20805796]

(8). Chugh P; Dittmer DP Potential Pitfalls in microRNA Profiling. Wiley Interdiscip. Rev. RNA 2012, 3 (5), 601–616. [PubMed: 22566380]

(9). Wang B; Howel P; Bruheim S; Ju J; Owen LB; Fodstad O; Xi Y Systematic Evaluation of Three microRNA Profiling Platforms: Microarray, Beads Array, and Quantitative Real-Time PCR Array. PLoS One 2011, 6 (2), e17167. [PubMed: 21347261]

(10). Lewis F; Maughan NJ; Smith V; Hillan K; Quirke P Unlocking the Archive - Gene Expression in Paraffin-Embedded Tissue. J. Pathol 2001, 195 (1), 66–71. [PubMed: 11568892]

(11). Siebolts U; Varnholt H; Drebber U; Dienes H-P; Wickenhauser C; Odenthal M Tissues from Routine Pathology Archives Are Suitable for microRNA Analyses by Quantitative PCR. J. Clin. Pathol 2009, 62 (1), 84–88. [PubMed: 18755714]

(12). Li J; Smyth P; Flavin R; Cahill S; Denning K; Aherne S; Guenther SM; O'Leary JJ; Sheils O Comparison of miRNA Expression Patterns Using Total RNA Extracted from Matched Samples of Formalin-Fixed Paraffin-Embedded (FFPE) Cells and Snap Frozen Cells. BMC Biotecnol 2007, 7, 36.

(13). Liu A; Tetzlaff MT; Vanbelle P; Elder D; Feldman M; Tobias JW; Sepulveda AR; Xu X MicroRNA Expression Profiling Outperforms mRNA Expression Profiling in Formalin-Fixed Paraffin-Embedded Tissues. Int. J. Clin. Exp. Pathol 2009, 2 (6), 519–527. [PubMed: 19636399]

(14). Doleshal M; Magotra AA; Choudhury B; Cannon BD; Labourier E; Szafranska AE Evaluation and Validation of Total RNA Extraction Methods for MicroRNA Expression Analyses in Formalin-Fixed, Paraffin-Embedded Tissues. J. Mol. Diagnostics 2008, 10 (3), 203–211.

(15). Xi Y; Nakajima GO; Gavin E; Morris CG; Kudo K; Hayashi K; Ju J Systematic Analysis of microRNA Expression of RNA Extracted from Fresh Frozen and Formalin-Fixed Paraffin-Embedded Samples. Rna 2007, 13, 1668–1674. [PubMed: 17698639]

(16). Tetzlaff MT; Liu A; Xu X; Master SR; Baldwin DA; Tobias JW; Livolsi VA; Baloch ZW Differential Expression of miRNAs in Papillary Thyroid Carcinoma Compared to Multinodular Goiter Using Formalin Fixed Paraffin Embedded Tissues. Endocr. Pathol 2007, 18 (3), 163–173. [PubMed: 18058265]

(17). Chen L; Li Y; Fu Y; Peng J; Mo M-H; Stamatakos M; Teal CB; Brem RF; Stojadinovic A; Grinkemeyer M; et al. Role of Deregulated microRNAs in Breast Cancer Progression Using FFPE Tissue. PLoS One 2013, 8 (1), e54213. [PubMed: 23372687]

(18). Yan L-X; Huang X-F; Shao Q; Huang M-Y; Deng L; Wu Q-L; Zeng Y-X; Shao J-Y MicroRNA miR-21 Overexpression in Human Breast Cancer Is Associated with Advanced Clinical Stage, Lymph Node Metastasis and Patient Poor Prognosis. RNA 2008, 14 (11), 2348–2360. [PubMed: 18812439]

(19). Weng L; Wu X; Gao H; Mu B; Li X; Wang J-H; Guo C; Jin JM; Chen Z; Covarrubias M; et al. MicroRNA Profiling of Clear Cell Renal Cell Carcinoma by Whole-Genome Small RNA Deep Sequencing of Paired Frozen and Formalin-Fixed, Paraffin-Embedded Tissue Specimens. J. Pathol 2010, 222 (1).

(20). Chapin SC; Appleyard DC; Pregibon DC; Doyle PS Rapid microRNA Profiling on Encoded Gel Microparticles. Angew. Chemie - Int. Ed 2011, 50 (10), 2289–2293.

(21). Chapin SC; Doyle PS Ultrasensitive Multiplexed MicroRNA Quantification on Encoded Gel Microparticles Using Rolling Circle Amplification. Anal. Chem 2011, 83 (18), 7179–7185. [PubMed: 21812442]

(22). Lee H; Shapiro SJ; Chapin SC; Doyle PS Encoded Hydrogel Microparticles for Sensitive and Multiplex microRNA Detection Directly from Raw Cell Lysates. Anal. Chem 2016, 88 (6), 3075–3081. [PubMed: 26863201]

(23). Le Goff GC; Srinivas RL; Hill WA; Doyle PS Hydrogel Microparticles for Biosensing. Eur. Polym. J 2015, 72, 386–412. [PubMed: 26594056]

(24). Dendukuri D; Gu SS; Pregibon DC; Hatton TA; Doyle PS Stop-Flow Lithography in a Microfluidic Device. Lab Chip 2007, 7 (7), 818–828. [PubMed: 17593999]

(25). Srinivas RL; Chapin SC; Doyle PS Aptamer-Functionalized Microgel Particles for Protein Detection. Anal. Chem 2011, 83, 9138–9145. [PubMed: 22017663]

(26). Montani F; Marzi MJ; Dezi F; Dama E; Carletti RM; Bonizzi G; Bertolotti R; Bellomi M; Rampinelli C; Maisonneuve P; et al. miR-Test: A Blood Test for Lung Cancer Early Detection. JNCI J. Natl. Cancer Inst 2015, 107 (6).

(27). Zhou J; Yu L; Gao X; Hu J; Wang J; Dai Z; Wang J-F; Zhang Z; Lu S; Huang X; et al. Plasma MicroRNA Panel to Diagnose Hepatitis B Virus–Related Hepatocellular Carcinoma. J. Clin. Oncol 2011, 29 (36), 4781–4788. [PubMed: 22105822]

(28). Yu L; Todd NW; Xing L; Xie Y; Zhang H; Liu Z; Fang H; Zhang J; Katz RL; Jiang F Early Detection of Lung Adenocarcinoma in Sputum by a Panel of microRNA Markers. Int. J. Cancer 2010, 127 (12), 2870–2878. [PubMed: 21351266]

(29). Chen Z-H; Zhang G-L; Li H-R; Luo J-D; Li Z-X; Chen G-M; Yang J A Panel of Five Circulating microRNAs as Potential Biomarkers for Prostate Cancer. Prostate 2012, 72 (13), 1443–1452. [PubMed: 22298030]

(30). Xing L; Todd NW; Yu L; Fang H; Jiang F Early Detection of Squamous Cell Lung Cancer in Sputum by a Panel of microRNA Markers. Mod. Pathol 2010, 23 (8), 1157–1164. [PubMed: 20526284]

(31). Dendukuri D; Pregibon DC; Collins J; Hatton TA; Doyle PS Continuous-Flow Lithography for High-Throughput Microparticle Synthesis. Nat. Mater 2006, 5 (5), 365–369. [PubMed: 16604080]

(32). DuPage M; Dooley AL; Jacks T Conditional Mouse Lung Cancer Models Using Adenoviral or Lentiviral Delivery of Cre Recombinase. Nat. Protoc 2009, 4 (7), 1064–1072. [PubMed: 19561589]

(33). Ambion. RecoverAllTM Total Nucleic Acid Isolation Kit: Protocol 2011.

(34). Lee H; Srinivas RL; Gupta A; Doyle PS Sensitive and Multiplexed on-Chip microRNA Profiling in Oil-Isolated Hydrogel Chambers. Angew. Chemie - Int. Ed 2015, 54 (8), 2477–2481.

(35). Kim JJ; Chen L; Doyle PS Microparticle Parking and Isolation for Highly Sensitive microRNA Detection. Lab Chip 2017, 17 (18), 3120–3128. [PubMed: 28815227]

(36). Tentori AM; Nagarajan MB; Kim JJ; Zhang WC; Slack FJ; Doyle PS Quantitative and Multiplex microRNA Assays from Unprocessed Cells in Isolated Nanoliter Well Arrays. Lab Chip 2018.

(37). Pregibon DC; Doyle PS Optimization of Encoded Hydrogel Particles for Nucleic Acid Quantification. Anal. Chem 2009, 81 (12), 4873–4881. [PubMed: 19435332]

(38). Schneider CA; Rasband WS; Eliceiri KW NIH Image to ImageJ: 25 Years of Image Analysis. Nat. Methods 2012, 9 (7), 671–675. [PubMed: 22930834]

(39). Hatley ME; Patrick DM; Garcia MR; Richardson JA; Bassel-Duby R; van Rooij E; Olson EN Modulation of K-Ras-Dependent Lung Tumorigenesis by MicroRNA-21. Cancer Cell 2010, 18 (3), 282–293. [PubMed: 20832755]

(40). Zhang J; Wang J; Zhao F; Liu Q; Jiang K; Yang G MicroRNA-21 (miR-21) Represses Tumor Suppressor PTEN and Promotes Growth and Invasion in Non-Small Cell Lung Cancer (NSCLC). Clin. Chim. Acta 2010, 411 (11–12), 846–852. [PubMed: 20223231]

(41). Stenvold H; Donnem T; Andersen S; Al-Saad S; Valkov A; Pedersen MI; Busund L-T; Bremnes RM High Tumor Cell Expression of microRNA-21 in Node Positive Non-Small Cell Lung Cancer Predicts a Favorable Clinical Outcome. BMC Clin. Pathol 2014, 14 (1), 9. [PubMed: 24524655]

(42). Higgs G; Slack F The Multiple Roles of microRNA-155 in Oncogenesis. J. Clin. Bioinforma 2013, 3 (1), 17. [PubMed: 24073882]

(43). Kasinski AL; Slack FJ miRNA-34 Prevents Cancer Initiation and Progression in a Therapeutically Resistant K-Ras and p53-Induced Mouse Model of Lung Adenocarcinoma. Cancer Res 2012, 72 (21), 5576–5587. [PubMed: 22964582]

(44). Grosso S; Doyen J; Parks SK; Bertero T; Paye A; Cardinaud B; Gounon P; Lacas-Gervais S; Noël A; Pouysségur J; et al. MiR-210 Promotes a Hypoxic Phenotype and Increases Radioresistance in Human Lung Cancer Cell Lines. Cell Death Dis 2013, 4 (3), e544–e544. [PubMed: 23492775]

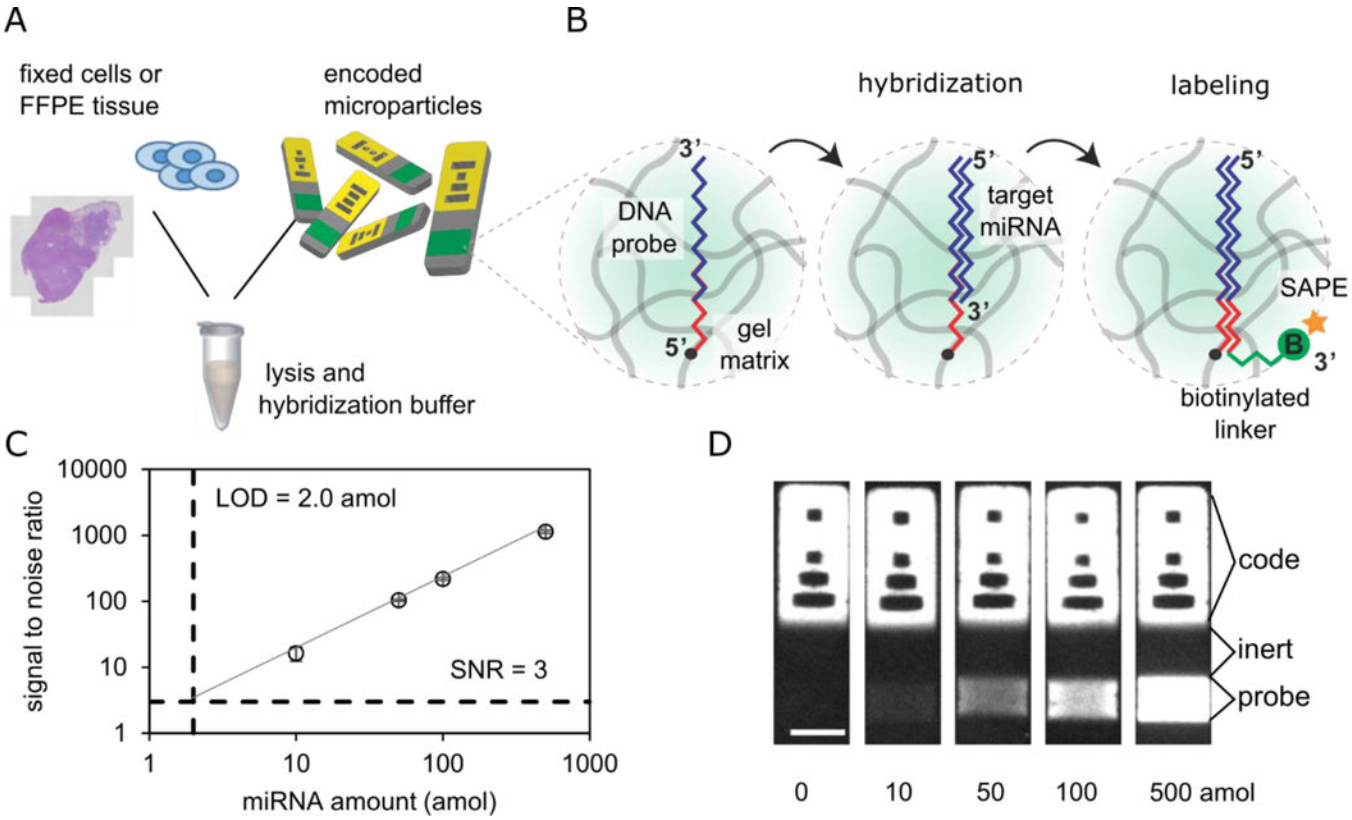

Figure 1.

(A) miRNA detecting hydrogel microparticles are added directly to fixed cells or FFPE tissue section in experiments in this paper. (B) Target miRNA hybridizes to probes on the particles, biotinylated adapter sequence is ligated to the end of the bound miRNA target, and streptavidin-R-phycoerythrin (SAPE) binds to biotin to allow fluorescence quantification. (C) Calibration curve for particles detecting miR-21, and (D) example particles from calibration curve. Scale bar 50 μm. Limit of detection (LOD) is 2.0 amol.Error bars = 1 standard deviation.

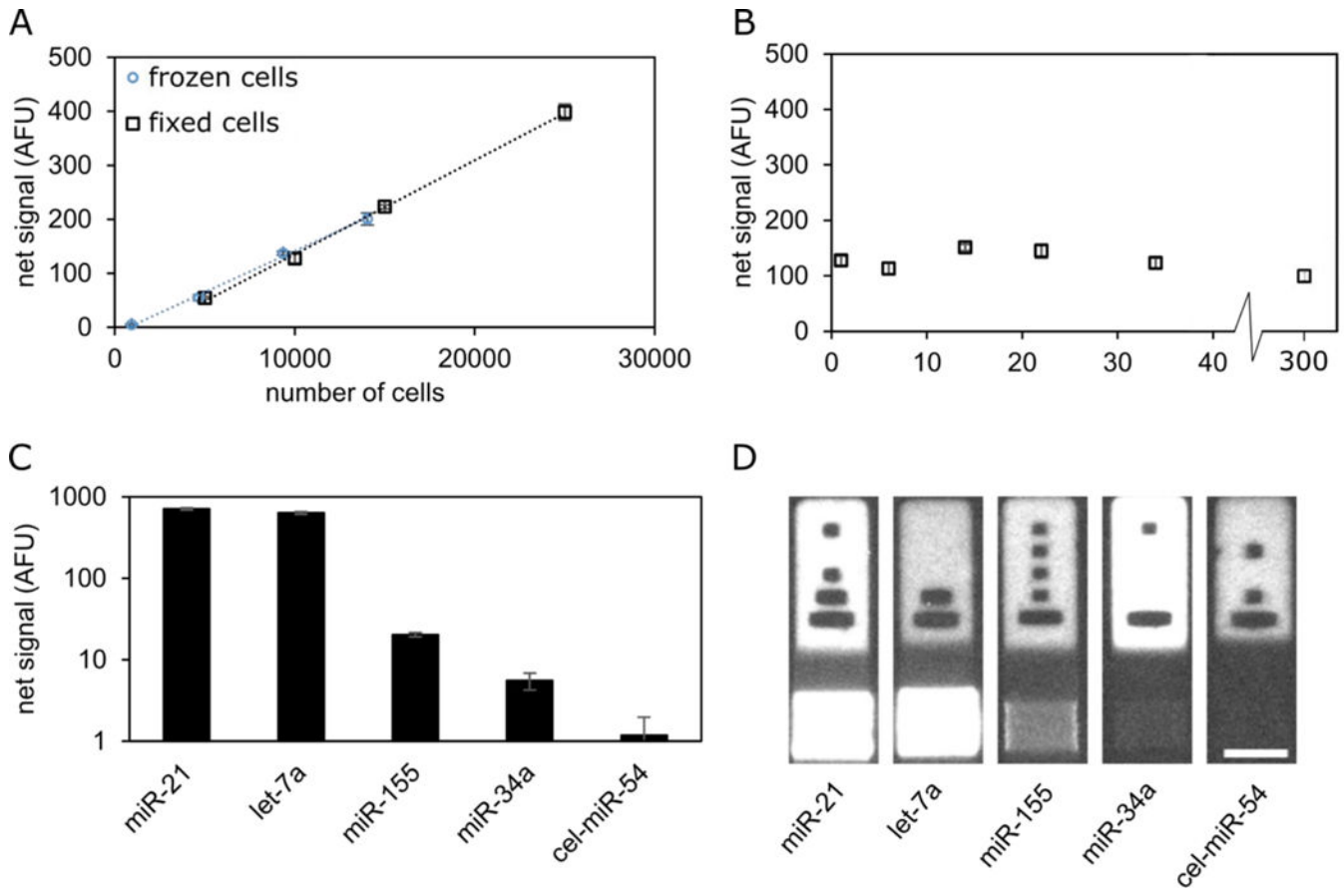

Figure 2.

Multiplexed miRNA quantification from frozen and fixed Calu-6 cells. (A) miR-21 quantification from frozen and fixed Calu-6 cells. (B) miR-21 quantification from 10,000 fixed Calu-6 cells as a function of time after initial fixation. (C) Multiplexed quantification from 70,000 Calu-6 cells. (D) Representative particles of the five different miRNAs tested. Scale bar 50 μm. Error bars = 1 standard deviation.

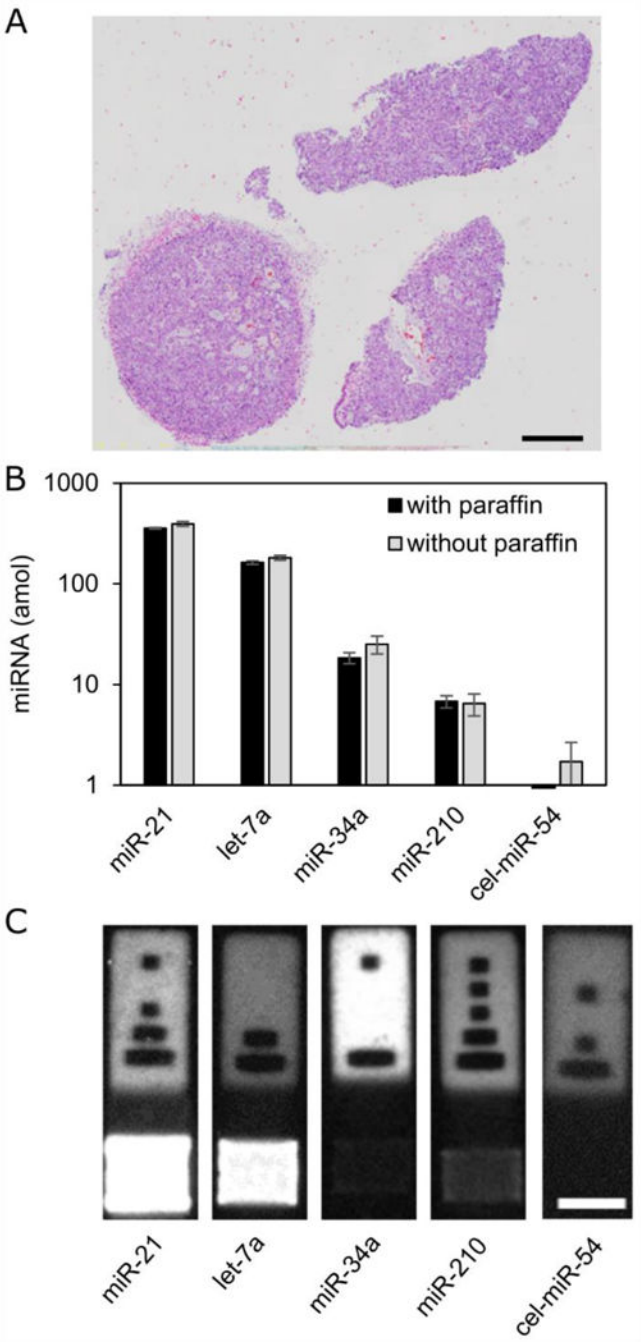

Figure 3:

Multiplexed miRNA quantification from FFPE tissue with paraffin and after paraffin was removed. (A) H&E stain of proximal tissue section. Scale bar 1 mm. (B) Results of quantification of 5 μm section with and without paraffin. (C) Representative particles from assay. Scale bar 50 μm. Error bars = 1 standard deviation.

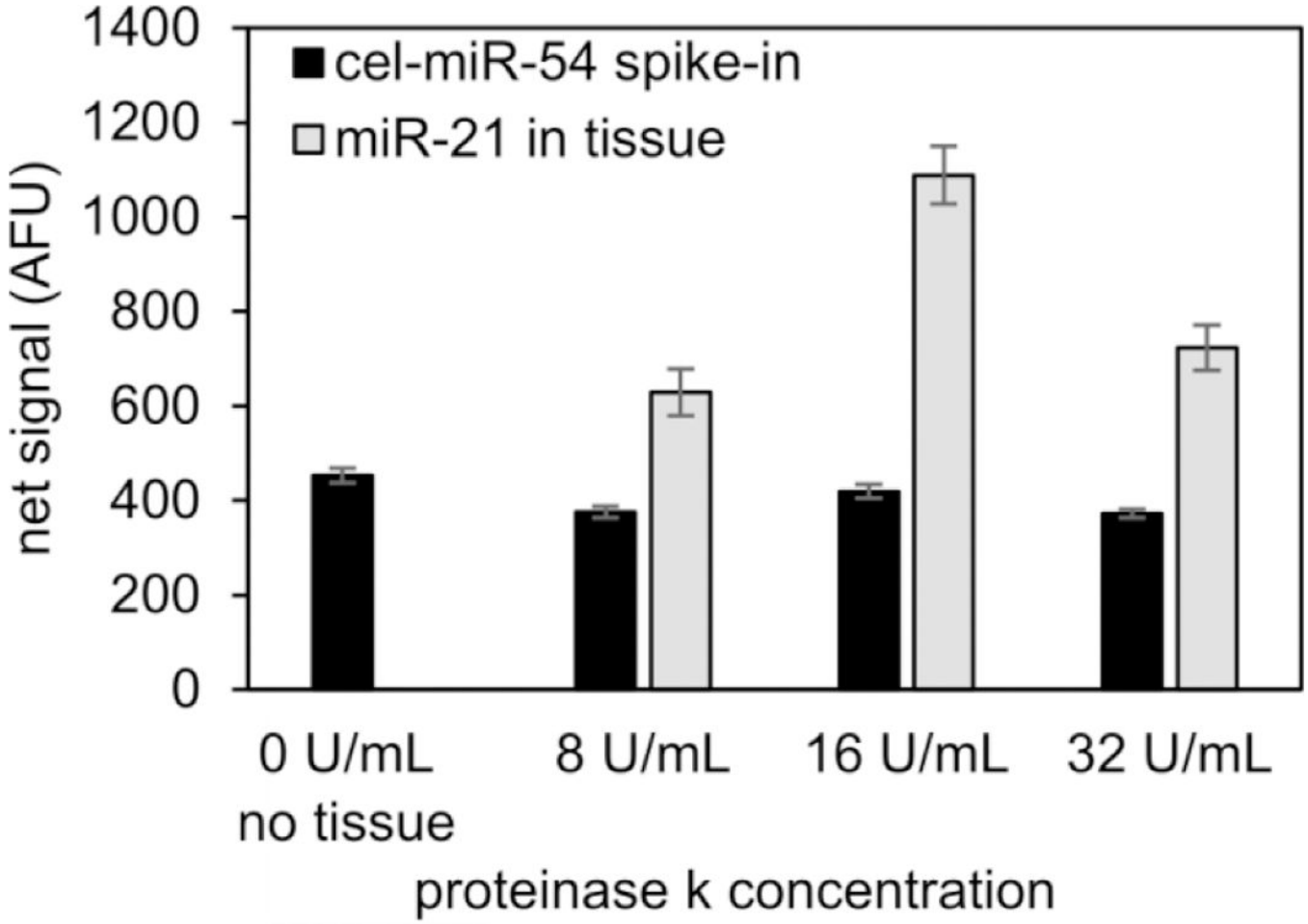

Figure 4:

Optimization of proteinase K in tissue assay. Signal of miR-21 (present in tissue) shows the effects of proteinase K on amount of miRNA released from tissue and measured by microparticles, while signal of *cel*-miR-54 (not present in tissue) shows the effects of proteinase K and tissue on miRNA assay performance. Error bars = 1 standard deviation.

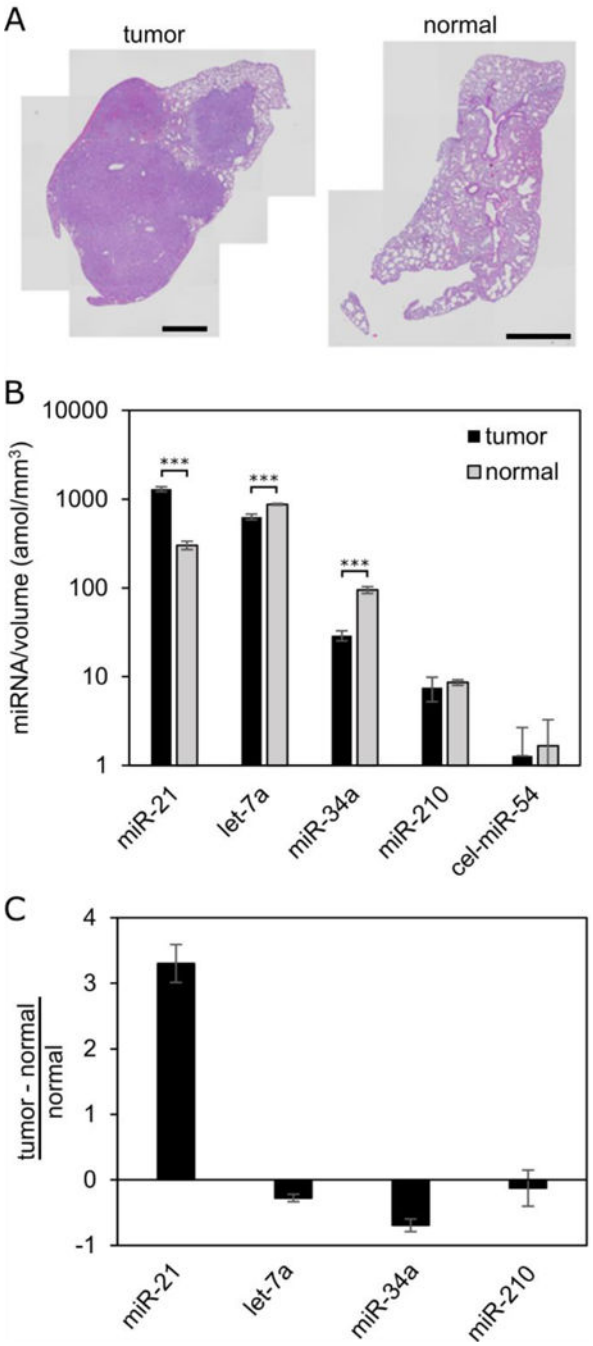

Figure 5:

Comparison of normal and tumor tissue sections with multiplexed miRNA assay. (A) H&E stains of the paired tumor (left) and normal (right) tissue sections in the same mouse from the *K-ras; p53* genetically engineered mouse model of non-small cell lung cancer. Scale bars 1 mm. (B) MiRNA signal normalized by volume of tissue for miR-21 (oncogenic miRNA[40]), let-7a and miR-34a (tumor suppressing miRNAs[2,43]), and miR-210 (hypoxia marker[44]). *** indicates $P < .001$ from two sample t-test. (C) Normalized differential

miRNA signal between tumor and normal tissue. *Cel*-miR-54 is quantified as a negative control. Error bars = 1 standard deviation.